

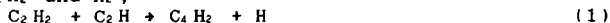
## Studies on The Reactions: $C_2H + C_2H_2 \rightarrow C_4H_2 + H$ AND $C_2H + H_2 \rightarrow C_2H_2 + H$

K. Fukuda, M. Koshi, and H. Matsui\*  
Department of Reaction Chemistry, The University of Tokyo  
7-3-1 Hongo, Bunkyo-ku, Tokyo 113, Japan

Key Words: Reactions of Ethynyl Radical, Shock Tube,  
Flash Photolysis

### 1. Introduction

Ethynyl radical ( $C_2H$ ) has been recognized as an important precursor of soot formation in the pyrolysis of acetylene and is also believed to be important in the formation of interstellar molecules. The rate constants of the elementary reactions of  $C_2H$  with  $C_2H_2$  and  $H_2$ ,



and



have been measured by several groups at room temperature, however, some disagreement among them were indicated<sup>1)-4)</sup>, also no direct data are available at high temperature range except for those based on indirect measurement on the pyrolysis of  $C_2H_2$ <sup>5)</sup>, or from speculative simulation<sup>6)</sup>.

As the flash photolysis with intense excimer laser radiation combined with shock wave heating technique has enabled us to get direct information on the details of radical reactions at high temperature range, the processes (1) and (2) have been examined in this study. In addition, flash photolysis studies at room temperature with a mass spectrometer have been performed to ensure the temperature dependences on these reaction processes at wider temperature range. Thus, the kinetic informations derived in this work may be very useful both in the fundamentals of chemical kinetics as well as in the numerical simulations of practical combustion systems.

### 2. Experimental System

The details of the experimental systems were described in our previous publications<sup>7), 8)</sup>. Two independent experimental systems have been used in this study: an excimer laser photolysis behind shock waves was used to study these reaction processes at elevated temperatures (above 1000 K), where, hydrogen atoms produced in the reactions were monitored by using atomic resonance absorption spectroscopy (ARAS), and an electron impact ionization mass spectroscopy was used to measure the rate constants and examine the reaction products at room temperature.

For the high temperature experiment, a diaphragmless shock tube of 5 cm i.d. made of stainless-steel was used. Sample gases were irradiated by an ArF laser (Questek V- $\beta$ , about 15 ns pulse duration) through a rectangular quartz window (4cmx1cm) located at the end plate after being heated by reflected shock waves.  $C_2H_2$  was photodissociated by the UV laser radiation to form  $C_2H$  and H. In the high temperature experiment, time dependence of H atoms produced in the photolysis (in the range of  $10^{11}$ - $10^{12}$

molecules/cm<sup>3</sup>) were monitored by an atomic resonance spectroscopic system (ARAS) at 121.6 nm. Absolute concentration of H atoms were decided by using a calibration curve which was decided by conducting thermal decomposition experiment using H<sub>2</sub>-N<sub>2</sub>O-Ar mixtures. The main advantage of the diaphragmless type shock tube is its excellent reproducibility of the shock heated condition: signal averaging at a fixed shock condition, when required, and plotting first-order rate against the concentration of the reacting partner in deciding the bimolecular rate constant were performed in this study to improve the quality of the kinetic informations.

The 193 nm photolysis experiment at room temperature was conducted in a slowly flowing pylex tube of 1.5 cm i.d. Sample gases were directly introduced into the vacuum chamber through a pinhole of 100 $\mu$ m i.d. and continuously detected by an electron-impact ionization mass spectrometer (Anelva TE 600-S). The ion signals from a secondary electron multiplier operated under pulse-counting conditions were recorded with a gated counter following pulse amplification and discrimination. Time dependence of the individual mass peak was obtained by scanning the delay time of the gate with the fixed gate width of 50 or 100  $\mu$ s. Signals were averaged over 10<sup>4</sup> laser shots for each run.

### 3. Experimental Results

Firstly, the reactions of C<sub>2</sub>H produced by an ArF laser photolysis in the mixtures of C<sub>2</sub>H<sub>2</sub> and C<sub>2</sub>H<sub>2</sub>+H<sub>2</sub> highly diluted in Ar were studied behind reflected shock waves. Typical oscillogram traces for the ARAS experiment behind shock waves are shown in Fig.3. The absorption intensity at 121.6 nm increased when shock waves passed through the observation section due to C<sub>2</sub>H<sub>2</sub>. With a proper delay time (typically 50  $\mu$ s) after the shock wave passage, ArF laser was fired and the rapid increment of the absorption intensity was observed by the production of H atoms by the photolysis of C<sub>2</sub>H<sub>2</sub>: then, the intensity gradually increased to a steady state with a single-exponential profile.

The detailed mechanisms for the photodissociation of C<sub>2</sub>H<sub>2</sub> by 193 nm laser has not been clarified yet. In this study, the rate of the increment of H atoms following the photolysis was not affected by the intensity of the ArF laser and, also the concentration of H atoms at steady state was always equal to about twice of that initially formed by the photolysis: moreover, the concentrations of the initial H atoms produced by the ArF laser photolysis was approximately proportional to the input laser energy, i.e., the ratio of (H) produced in the flash photolysis to the initial concentration of C<sub>2</sub>H<sub>2</sub>, (H)/(C<sub>2</sub>H<sub>2</sub>)<sub>0</sub> varied from about 0.15% to 1% for the input laser powers of 10 to 60 mJ/cm<sup>2</sup> over the temperature range of 1000-2000 K. Thus, the multiphoton process that lead to the production of C<sub>2</sub>+2H was concluded to be unimportant at this input energy range<sup>1)</sup>. It was also confirmed that the rise rates of H atoms were proportional to both the initial concentration of C<sub>2</sub>H<sub>2</sub> and that of added H<sub>2</sub>, as are shown in Fig.4 and Fig.5.

Based on these experimental evidences, it was assumed that the

initial concentration of H atoms produced by the 193 nm photolysis was equal to that of  $C_2H(X^2\Sigma^+)$  at the present experiment: the quenching rate of the possible electronically excited  $C_2H(A^2\Pi)$  produced in the photolysis was supposed to be sufficiently fast in the time scale of the shock wave experiment. Thus, the informations on the time dependence of H atoms should be directly related to those for (1) or (2): the rate constants for these processes were evaluated from the slopes of the plot of the first order rate against initial concentrations of  $C_2H_2$  and  $H_2$  shown in Fig.4 and Fig.5, respectively.

The results are summarized as,  $k_1 = (6.6 \pm 1.1) \times 10^{-11}$  ( $cm^3$  molecule $^{-1}$  s $^{-1}$ ) over  $T = 1260$ - $2487$  K without appreciable temperature dependence, and  $k_2 = (3.3 \times 10^{-10}) \exp(-13.8 \text{ kcal mol}^{-1}/RT)$  ( $cm^3$  molecule $^{-1}$  s $^{-1}$ ) over  $T = 1565$ - $2218$  K. In order to check the sensitivity of the side reactions in these experimental conditions, numerical computations including 11 elementary reactions were performed at some typical experimental runs; no effective contribution from the side reactions was found in evaluating  $k_1$  and  $k_2$ .

The reaction processes (1) and (2) were examined by the 193 nm photolysis also at room temperature, where the time dependent concentration of  $C_4H_2$  was monitored by an electron-impact mass spectrometer with an electron energy of 20 eV.

For the experiment on  $C_2H_2$ -Ar mixtures, as is shown in Fig.6, when  $C_2H_2$  was irradiated by 193 nm, the concentration of  $C_4H_2$  ( $m/e = 50$ ) increased exponentially towards steady level, and the rise rate of it linearly depended on the initial concentration of  $C_2H_2$ . From the slope shown in this figure, the rate constant was decided as,  $k_1 = 4.6 \times 10^{-11}$  ( $cm^3$  molecule $^{-1}$  s $^{-1}$ ) at 293 K. This value is consistent with that at high temperature range.

When sufficient amount of  $H_2$  was added to the  $C_2H_2$ -Ar mixtures, the rise rate of  $C_4H_2$  became too large to decide the rate constant for (2) accurately. However, the experimental conditions were chosen so that the effect of the side reactions except (1) and (2) could be neglected (as was already noted above), then the reaction rate constant for (2) could be decided by measuring the steady state concentration of  $C_4H_2$ ,  $(C_4H_2)_s$ , with the following relation,

$$(C_2H)_s / (C_4H_2)_s = 1 + (k_2/k_1)(H_2)/(C_2H_2) \quad (3)$$

where,  $(C_2H)_s$  is the initial concentration of  $C_2H$  produced by the ArF photolysis. Fig.7 shows the validity of this relation. The experiment was conducted with 0.63 and 0.74 Torr partial pressure of  $C_2H_2$  and the energy of 193 nm laser was fixed to 12 mJ/cm $^2$ , where, the pressure of  $H_2$  was varied from 0 to 310 mTorr: the rate constant for (2) estimated from the slope of this plot was,  $k_2 = 4.83 \times 10^{-14}$  ( $cm^3$  molecule $^{-1}$  s $^{-1}$ ) at 293 K.

#### 4. Discussion and Comparison with The Previous Results

The present results on  $k_1$  together with the previous ones are summarized in Fig.8. The present results agree well with that by Frank and Just $^5$  at high temperature range and also with those by Lange and Wagner $^2$  and Laufer and Bass $^1$  at room temperature: it is not clear why only the rate constant measured by Stephens et

al.<sup>11</sup> who monitored the concentration of  $C_2H$  by color centered laser was about 5 times faster than the previous studies<sup>2, 3, 7</sup> or present result. They attributed this difference of the rate constants to the formation of the intermediate species, however, more direct evidence may be required to support this mechanism.

The other important reaction in the initiation stage of  $C_2H_2$  pyrolysis (2) has been studied by several groups but the rate constant of it shows substantial disagreement each other<sup>1, 2, 3, 7</sup>; the reaction intermediate was discussed in order to explain the difference between the rate of reactant and products. As can be seen in Fig.9, the present result on  $k_2$  at room temperature was smaller than the previous ones. This process is supposed to have substantial temperature dependence because of the energy barrier of the transition state. No direct experimental data at high temperature are available, although some speculative rate constant has been used in the computer simulations<sup>8, 9</sup>. The rate constant suggested in the previous works has shown highly non-Arrhenius temperature dependence. Our results at high temperature range has considerably large temperature dependence, thus, the extrapolation of them to the room temperature range gives much smaller rate constant than those directly measured. Such non-Arrhenius temperature dependence of the rate constant for (2) was discussed by Harding et al. based on transition state properties of  $C_2H$  estimated by ab initio calculation<sup>10</sup>. Although the observed activation energy in this study (13.8 kcal/mol) was much larger than that estimated in POL-CI calculation (4.0 kcal/mol), the TST theory seems consistent with the present experiment: it is suggested that the large temperature dependence of the rate constant for (2) was brought both by the temperature dependence of vibrational partition function of the transition state (high temperature range) and tunneling effect (low temperature range).

#### References

1. J.W. Stephens, J.L. Hall, H. Solka, W.B. Yan, R.W. Curl, G.P. Glass, *J. Chem. Phys.*, **91** 5740 (1987)
2. W. Lange and H.G. Wagner, *Ber. Bunsenges. Phys. Chem.*, **79** 165 (1975)
3. A.H. Laufer and A.M. Bass, *J. Phys. Chem.*, **83**, 310 (1979)
4. A.M. Renlund, F. Shokoohi, H. Reisler, and C. Wittig, *Chem. Phys. Lett.*, **84** 293 (1981)
5. P. Frank and Th. Just, *Comb. Flame* **38** 231 (1980)
6. W. Tsang and R.F. Hampson, *J. Phys. Chem. Ref. Data*, **15** 1087 (1986)
7. M. Koshi, M. Yoshimura, K. Fukuda, and H. Matsui, *J. Chem. Phys.*, **93** 8703 (1990)
8. M. Koshi, A. Miyoshi, and H. Matsui, *Chem. Phys. Lett.* (under submission)
9. T.A. Cool, P.M. Goodwin, and C.E. Otis, *J. Chem. Phys.*, **93** 3714 (1990)
10. L.B. Harding, G.C. Schatz, and R.A. Chiles, *J. Chem. Phys.*, **76** 5172 (1982)

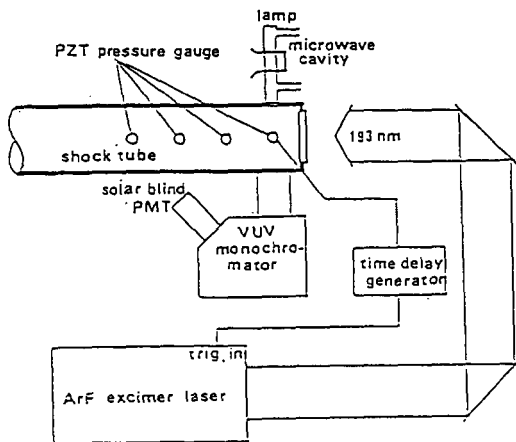


Fig.1 A schematic of the shock tube - laser flash photolysis system used in the high temperature experiment

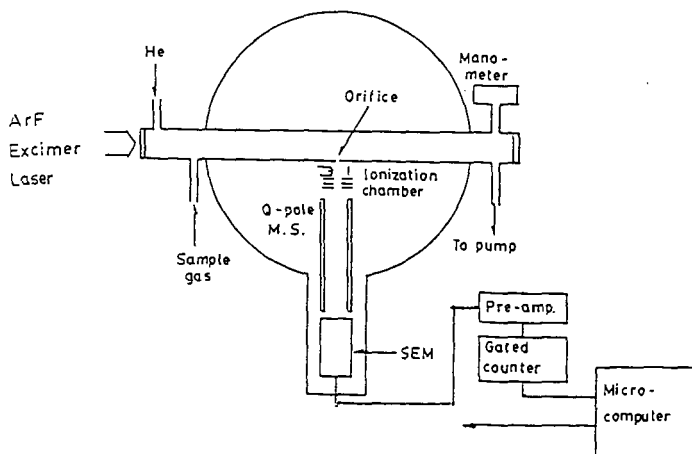


Fig.2 A schematic of the laser photolysis - mass spectrometer system used in the room temperature experiment

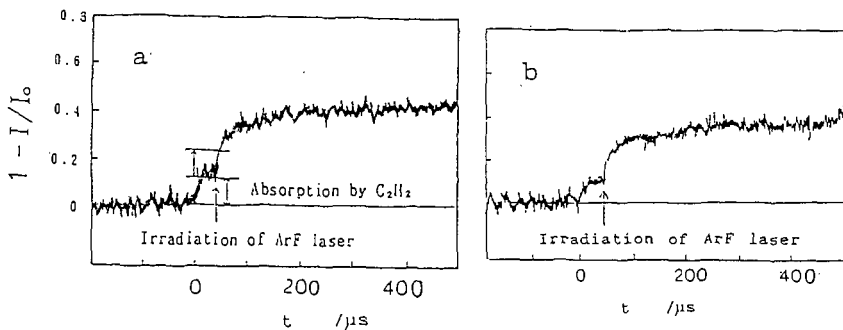


Fig.3 Examples of oscillogram trace of 121.6 nm absorption in ArF photolysis behind reflected shock waves  
 a: 86 ppm  $C_2H_2$  in Ar,  $T = 1758$  K,  $p = 1.92$  atm.  
 b: 21 ppm  $C_2H_2$  + 400 ppm  $H_2$  in Ar,  $T = 1639$  K,  $p = 1.33$  atm.

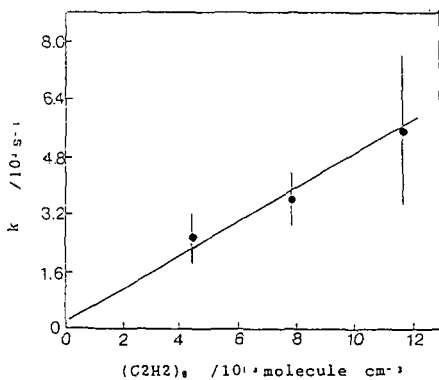


Fig.4 Dependence of the rate of increment of H atoms on the initial concentration of  $C_2H_2$  ( $T = 1640 \pm 20$  K,  $p_1 = 20$  Torr, 30-150 ppm  $C_2H_2$  diluted in Ar)

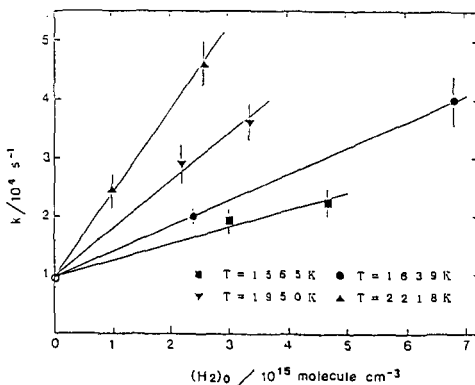


Fig.5 Dependence of the rate of increment of H atoms on the initial concentration of  $H_2$  (21 ppm  $C_2H_2$  + 400-1100 ppm  $H_2$  diluted in Ar,  $p_1 = 20$  Torr)

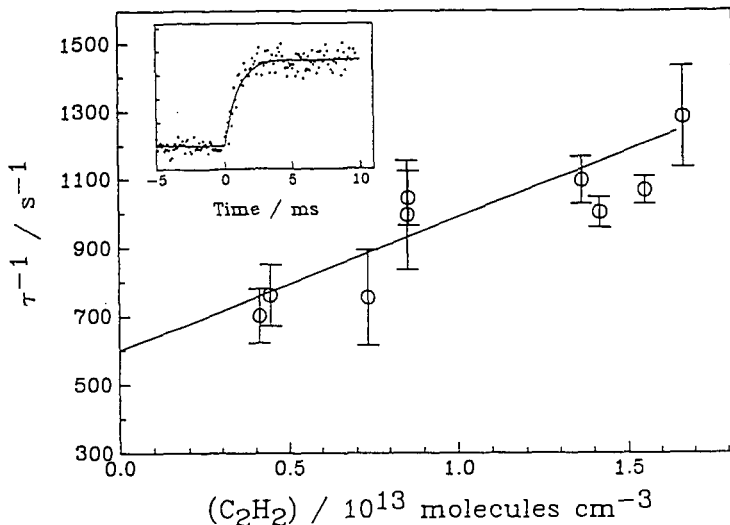


Fig. 6 First order production rates of  $C_4H_2$  as a function of  $C_2H_2$  concentrations. A time profile shown in the figure was taken with  $(C_2H_2)_0 = 8.6 \times 10^{12}$  molecules/cm<sup>3</sup>.

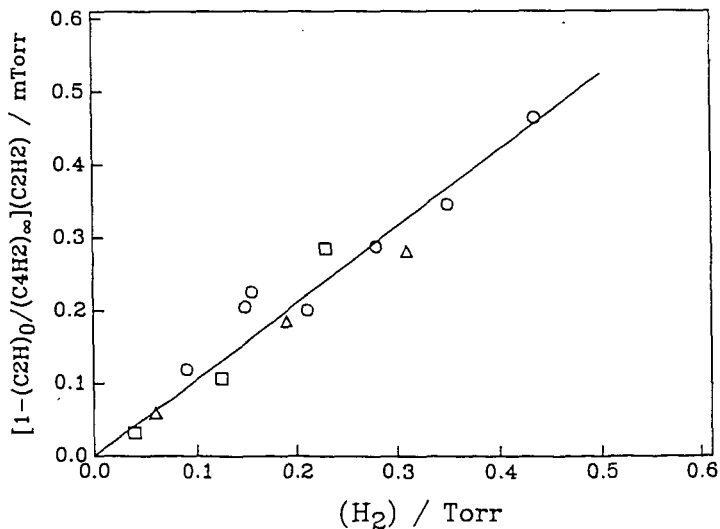


Fig. 7 Plot of  $[1 - (C_2H)_0 / (C_4H_2)_\infty] (C_2H_2)$  vs  $(H_2)$ . Slope of this plot is equal to  $k_2/k_1$  (see Eq.(3)). O;  $(C_2H_2) = 0.24$  mTorr, □;  $(C_2H_2) = 0.63$  mTorr, Δ;  $(C_2H_2) = 0.74$  mTorr.

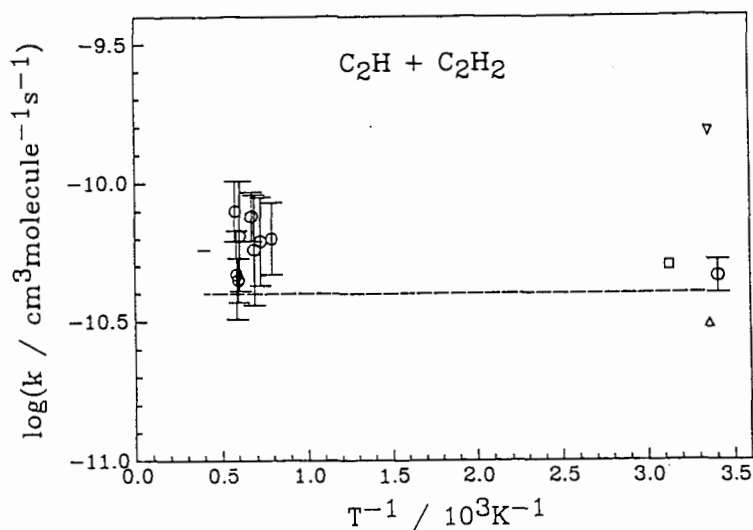


Fig.8 Arrhenius plot for the rate constant of the  $C_2H + C_2H_2 \rightarrow C_2H_2 + H$  reaction.  $\bigcirc$ ; This work,  $\nabla$ ; ref.1,  $\square$ ; ref.2,  $\triangle$ ; ref.3,  $-$ ; ref.5,  $- -$ ; ref.6.

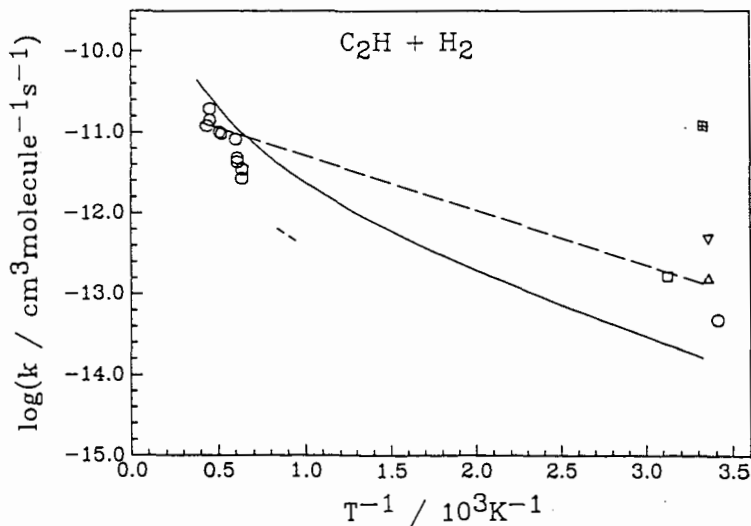


Fig.9 Arrhenius plot for the rate constant of the  $C_2H + H_2 \rightarrow C_2H_2 + H$  reaction.  $\bigcirc$ ; This work,  $\nabla$ ; ref.1,  $\square$ ; ref.2,  $\triangle$ ; ref.3,  $\boxtimes$ ; ref.4,  $- -$ ; ref.6. A solid curve is a result of TST calculation with parameters given in ref.10.